

Geochemical and Petrological characteristics of the Granitoid Complex of Boroujerd, Western Iran

Zahra Khodakarami Fard¹, Reza Zarei Sahameih² and Ali Khodakarami Fard^{3*}

- 1- Research evaluation superintendent, Research and Technology Vice Chancellorship of the Lorestan University of Medical Sciences, Khorramabad, Iran and Graduated M.S of Geology , Islamic Azad University of Khorramabad Branch, Iran
- 2- Department Of Geology, Faculty of Science, Lorestan University, Khorram Abad, Iran
- 3- M.S. Student Geologic Remote Sensing, Islamic Azad University of Khorramabad Branch, Iran

Corresponding author: Ali Khodakarami Fard

ABSTRACT: The Granitoid Complex of Boroujerd belongs to the Sanandaj-Sirjan Zone (SSZ) in the western of Iran. It is elongated and parallel to the prevailing schistosity in the metamorphic rocks by the trend of NW–SE and consists of quartz diorites, granodiorites, monzogranites and acidic dikes (aplites and pegmatites). This Complex is of sub-alkaline affinity; belong to the high-K calc-alkaline series, metaluminous to weakly peraluminous, and display features typical of I-type granites.

Trace and rare-earth elements distribution patterns for the Boroujerd granitoid rocks indicate a distinctive depletion with respect to primitive mantle in Nb, Eu, Sr, Ba, P and Ti relative to other trace elements and a greater enrichment in LILE compared to HFSE. These geochemical characteristics suggest that these rocks derived from a crustal source.

The granitoid Boroujerd has geochemical characteristics typical of arc intrusives and plot as volcanic arc granites on various discriminant diagrams. This granitoid is typical representatives of a volcanic arc environment, spatially related to an active continental margin. Probably, it is the result of the subduction of Neo- Tethyan oceanic crust below the Iranian microcontinent. All available data are compatible with the idea that these rocks represent the products of convergent margin processes during the Mesozoic.

Keywords: Iran , I-type granite, continental arc, Neo- Tethyan.

INTRODUCTION

The Sanandaj-Sirjan Zone, which host the Boroujerd granitoid complex, has a length of 1500 km and a width up to 200 km from northwest to southeast of Iran (Fig. 1). This tectonic zone is mainly composed of Mesozoic and some Paleozoic rocks (Berberian, 1977) and separates the stable Central Iran block, from the Afro-Arabian plate (Stöcklin, 1968).

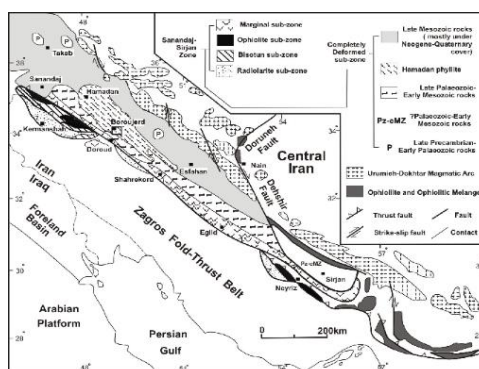


Figure 1. Tectonic sketch map of western Iran after Mohajjel et al. 2003 showing location

Berberian (1983) considered this zone as a Mesozoic magmatic arc, and a Tertiary fore-arc. Presence of a narrow arc-trench gap in this belt is an indication of steep subduction (Isacks and Barazangi, 1977; Berberian and Berberian, 1981). The Sanandaj-Sirjan calc-alkaline magmatic arc, including the Boroujerd complex, formed over a high angle subducting oceanic slab in the Neotethyan subduction zone during late Triassic to late Cretaceous time (e.g., Berberian and Berberian, 1981; Shahabpour, 2005).

The main aims of this paper is to present geochemical characters, as well as observed field relationships of the Boroujerd complex, to characterise granite magmatism, determine its origin and tectonic environment in the Sanandaj-Sirjan Zone and to shed light on the Alpine history and related magmatism in Iran. The data in this paper are important for the understanding of the presence of a subduction zone in SW of Iran during the Mesozoic.

2. Geological setting

The Boroujerd granitoid complex is a NW-SE trending body covering an area of 600 km², approximately 60 km in length and 8-10 km in width, which lies between 33° 38' - 34° N and between 48° 45' - 49° 20' E (Fig. 2). The Boroujerd area is characterised by the predominance of metamorphic rocks of Jurassic age (Baharifar et al, 2004) and the Boroujerd huge granitoid complex. Metamorphic rocks subdivided to 3 groups based on their setting: Dynamothermal, Contact and Retrograde. Dynamothermal metamorphism has affected a vast area and is composed of slate, phyllite, schist, Meta volcanic and tuff, Meta cherty limestone and Meta sandstone (Ahmadi Khalaji, 2006). By the injection of large granitoid pluton, a contact metamorphism has occurred which can be considered as a pyroxene hornfels facies. Contact metamorphism rocks consist of spotted schist, hornfels schist, cordierite-, andalusite-cordierite-, sillimanite hornfelses (Ahmadi Khalaji, 2006). The contact metamorphism of the northern margin is better developed and exposed than those of the southern margin. This suggests that the southern contact of Boroujerd complex is controlled by a fault system parallel to the contact (Berthier, 1974; Masoudi, 1997).

U-Pb zircon geochronological data from a variety of granitoid rocks, including the main units and associated pegmatitic dikes, indicate a strong, but short-lived episode of magmatic activity during the period 172 Ma to 169 Ma in the middle Jurassic (Ahmadi Khalaji, 2006). The ages of the granitoid Complex are indistinguishable from the timing of emplacement of the late stage pegmatitic dikes which represent the final stages of magmatism.

3. Petrography

Boroujerd granitoids include quartz diorite, granodiorite and monzogranite. They cut by numerous acidic dikes. The granodiorites are widespread throughout the area and the biggest intrusion in the area with an elongate shape extending north-west (Fig. 2). They are gray and generally medium to coarse-grained rocks and have a granular to weakly porphyritic texture showing a simple mineralogy: Plagioclase (30-40 % mod.), K-feldspar (<10 % mod.), Quartz (25-30 % mod.) and Biotite (10-20 % mod.). Apatite, zircon and allanite occur in all samples (0.5–1.6 % mod.).

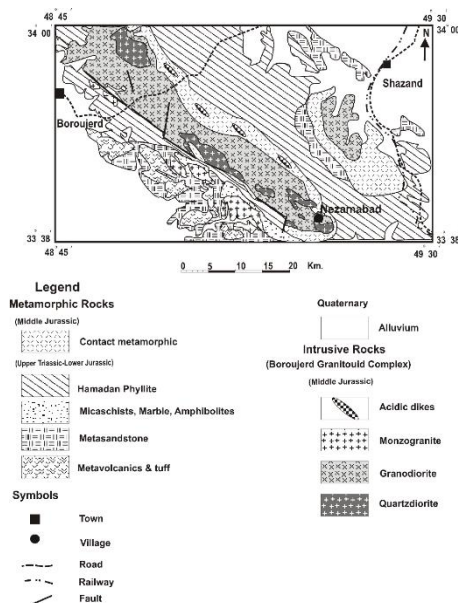


Figure 2. Geological map of the Boroujerd Granitoid Complex

Fine-grained microgranodioritic enclaves are abundant in these rocks. Their size is variable with average lengths of 10-30cm. Their mineralogy and texture is similar to the host granodiorite. Enclave shapes are globular, ellipsoid or rounded and are fragments of chilled margins. These enclaves have a co-magmatic nature with their host.

The quartz diorites are exposed within the granodiorites and have diffuse boundaries with them. These rocks have granular texture to porphyritic with plagioclase megacrysts and composed predominantly of plagioclase (40-50% mod.), amphibole (5-10% mod.), biotite (15-20% mod.), alkali feldspar (<5% mod.) and quartz (<10% mod.). Zircon, sphene, apatite are common accessory minerals.

The monzogranites widely scattered as separate and small outcrops through the southern part (Fig. 2). These rocks are light in colour and fine to coarse-grained (fine grain in margin and coarse grain in center) and display a porphyritic texture (in center) with feldspar megacrysts and a granular texture in margin.

The mineral assemblages include perthitic alkali feldspar (20-25% mod.), plagioclase (15-25% mod.), quartz (30-35% mod.), biotite (7-10% mod.) and minor muscovite. Zircon, allanite, apatite are common accessory minerals.

Fine-grained microgranitic enclaves occur in these rocks. Their size is 5-15cm in length. Their mineralogy and texture is similar to the host. Enclave shapes are globular, ovoid or rounded and are fragments of chilled margins.

The granitoids are cut by a series of north-northwest trending aplites and pegmatites. The aplites are characterised by an equigranular texture of quartz, alkali feldspar, muscovite, tourmaline and opaque oxides. Pegmatites are mainly present in the granodiorites and their aureole. They show simple mineralogy and graphic texture. They are characteristically composed of quartz, feldspar, muscovite, tourmaline, zircon, apatite, garnet and andalusite. These rocks are the last differentiation product of granitoid magmas.

So, the Boroujerd granitoids consist of two different suites (types); a monzogranitic (more felsic, leucocratic type), and a quartz dioritic to granodioritic (more mafic or mesocratic type). Whereas the mesocratic type occurs as an ellipsoid large intrusion and form elongated SE-NW trending complexes, leucocratic type as small intrusions show round shapes suggesting a change in the crustal stress field

MATERIALS AND METHODS

About 300 samples of the granitoid rocks were collected from different facies. In order to correctly characterise their chemical compositions, 34 least-altered samples were chosen for major, trace and rare-earth-elements (REE) analysis. Major and trace element abundances were determined by inductively coupled plasma atomic emission spectrometry (ICP-AES) and inductively coupled plasma-mass spectrometry (ICP-MS) at the ALS Chemex laboratories in Vancouver, Canada. The analytical processes are described in Cotten et al. (1995). The results of the analyses are reported in Table 1.

Table 1 . Major and trace element contents from the Borrower Granitoid Complex

Sample	Granodiorites													
	W30	A200	Q195	A201	Q2	Q4	Q5	A206	B1955	A04	A075	B4919		
SiO2	71.4	70.8	67.2	64.9	64.3	63.6	63.4	62.6	60.6	59.7	58.5	57.3		
TiO2	0.3	0.3	0.5	0.5	0.6	0.6	0.6	0.7	0.7	0.8	1	1		
Al2O3	14.7	14.5	15.6	16	16.7	16.9	16.1	16.9	17.5	20.2	19	18.3		
Fe2O3tot	1	2.6	2	4.5	5.5	5.6	6.2	6.7	6.6	4.3	8	8.7		
MnO	0	0.1	0	0.3	0.1	0.1	0.1	0.1	0.1	0	0.1	0.1		
MgO	2.9	3.9	3.9	1.4	1.6	1.6	1.6	1.8	1.8	1.3	2.4	2.5		
CaO	0.3	2.2	0.7	2.5	3.9	3.8	3.8	3.8	4.1	5.2	4.1	4.3		
Na2O	4.8	3	4.2	3.1	3.1	3	2.9	3.4	2.9	3.6	2.5	2.6		
K2O	1.3	4.1	1.4	4	3.4	3.6	3.4	3	3.4	3.4	3.2	3.3		
P2O5	0.1	0.1	0.2	0.3	0.2	0.1	0.1	0.2	0.3	0.2	0.4	0.1		
Na	12	13	19	19	17	16	19	21	22	16	32	47		
Cr	30	128	43	156	126	120	96	116	190	100	180	180		
Ce	55.3	6.4	41.9	10.2	12	11.1	11.1	11.8	12.6	8.9	16.6	19.6		
V	31	36	55	60	88	88	61	78	57	58	155	152		
Co	0.5	5.2	0.9	9.3	3.8	3.5	3	4.5	5.8	4.3	4.1	4.7		
Rb	40.8	142.5	29.3	146	130.5	133.5	122	111	134.5	133.5	129.5	142.5		
Sr	26.9	230	65.9	256	222	309	295	320	336	404	294	330		
Ba	80.2	441	173.5	577	596	596	551	549	765	1190	763	893		
U	23	24	23	21	12	10	17	32	2	14	15	25		
Th	2.2	2.7	1.6	1.9	2.4	3.3	2.5	2.3	1.4	2.3	1.9	2.2		
Ta	1.5	1.1	1.2	1	0.9	1	0.9	1	0.9	0.8	0.9	1		
Nb	15	12	16	14	14	13	14	17	15	15	19	21		
La	52.3	49.7	38.6	47.3	29.4	44.2	43.7	62.1	19.5	64	51	76.4		
Ce	94.1	93.6	62.2	91.1	69.9	92.6	82.5	104.5	48.8	118.5	103	155		
Pr	10.6	10	6	9.6	6.4	9.3	6.6	11.8	4.1	11.6	11	16.2		
Nd	35.8	33.1	21.2	32.3	22.4	31	30	40.9	15.1	38.6	38.2	56.6		
Sm	6.3	6.6	3.9	6.3	4	4.8	5.2	5.9	2.3	6.2	7	9.4		
Eu	0.6	1.2	0.2	1.2	1	1.1	0.9	0.9	1.3	2.2	1.3	0.8		
Gd	5.7	6.6	3.7	6	4.1	4.3	4.7	5.9	2.2	6.3	6.8	8.3		
Tb	0.8	0.8	0.5	0.7	0.5	0.6	0.6	0.6	0.2	0.8	0.9	1		
Dy	4.5	5.1	2.7	3.8	2.9	3.4	3.6	3	1.1	3.6	5.3	6.3		
Ho	0.9	1	0.6	0.7	0.6	0.7	0.7	0.6	0.2	0.6	1.1	1.4		
Er	2.8	3.1	1.6	2	2.1	2.1	2	1.6	0.7	1.2	3.6	4.5		
Tm	0.4	0.4	0.2	0.2	0.3	0.3	0.3	0.2	0.1	0.1	0.5	0.6		
Yb	2.7	2.9	1.5	1.7	2	2.3	1.8	1.4	0.7	0.8	3.4	4.5		
Lu	0.4	0.4	0.2	0.2	0.3	0.4	0.3	0.2	0.1	0.1	0.5	0.6		
Zr	27.8	27.2	16.2	19.2	18.8	20.2	19.6	13.6	6.7	15	21.6	27.4		
Hf	5	5	3	4	5	5	5	7	3	9	9	9		
Zr	147.5	162.5	230	179.5	203	203	198.5	227	232	341	274	287		
Hf	10	27	10	43	56	62	51	48	68	53	83	124		
Ga	15	17	15	21	22	20	21	20	20	26	22	26		
Se	2	2	2	2	1	1	1	2	2	2	2	2		
W	550	5	420	15	6	9	4	7	8	5	13	9		
Eu/Eu*	0.3	0.6	0.2	0.7	0.8	0.7	0.6	0.5	1.8	1.1	0.6	0.3		
ΣREE	12	11.2	12.7	18.6	9.8	12.9	15.1	29.7	18.6	53.5	19	11.4		

Table 1 (Continued)

Sample	Quartz dikes										
	G14	G16	G18	G19	EA201	GM05	G12	G11	AG2	EA26	EA23
SiO ₂	63.4	60.7	59.9	59.2	58.9	57.9	58.3	58.5	55.4	53.2	52.8
TiO ₂	0.6	0.6	0.6	0.8	0.7	0.8	0.9	0.7	1.3	0.7	0.6
Al ₂ O ₃	16.6	14.9	15.4	15.9	15.2	15.3	17.1	15.9	16.8	15.6	15.2
Fe ₂ O ₃ *	5	5.4	6.5	7.1	7.1	6.9	8	7.5	6.6	6.7	6.7
MnO	0.1	0.1	0.1	0.1	0.1	0.1	0.2	0.2	0.2	0.2	0.2
MgO	3.3	4.3	4.6	4.8	4.7	6.5	5.1	6.5	4.6	7.6	6.4
CaO	5.6	5.2	5.6	5.5	5.9	6.1	6.9	6.4	7.3	7.8	6.9
Na ₂ O	1.4	2.2	2.3	2.4	2.5	2.4	2.5	2.5	2.7	2.3	1.9
K ₂ O	2.3	3.5	3	2.8	2	2.5	2.1	2.2	1.8	2.1	1.8
P ₂ O ₅	0.2	0.1	0.1	0.2	0.1	0.1	0.2	0.1	0.3	0.1	0.1
Ni	37	53	57	63	49	115	75	101	38	66	103
Cr	260	280	260	330	330	420	380	450	150	490	690
Co	20	20.3	20.6	22.9	23.8	48	27.8	28.7	54.5	31.9	36.4
V	176	144	144	145	150	170	204	210	166	217	274
Cs	9.9	5	6.2	7.5	4.7	10	5.4	4.6	4.2	3.2	3.5
Rb	103	128	106	111	77.4	106.5	88.2	101	66.6	78.8	65.9
Sr	299	263	269	261	231	347	347	388	334	197	202
Ba	242	586	388	372	361	407	355	454	296	236	238
Th	4	24	7	13	5	11	9	10	7	5	5
U	2.5	3	2	1.8	2.3	2.1	2.4	2.6	1.9	1.4	1.2
Ta	0.8	1	0.9	0.9	0.9	0.9	0.9	0.7	1.1	0.5	0.5
Nb	8	12	10	12	10	10	12	9	13	7	8
La	13.8	68.3	79.4	33.8	15.4	28.8	27.2	24.1	79	16.6	20
Ce	32.9	146.5	44.2	72.3	41.5	65.5	57.6	50.1	44.4	38.4	50.7
Pr	3.9	14.9	5.4	7.9	5.7	6.7	6.7	5.8	5.1	4.4	5.1
Nd	14.8	49.4	20.9	26.7	26	24	25	21.8	19.8	16.2	23.9
Sm	3.9	8.3	4.4	5.6	5.4	4.8	5	4.4	4.8	3.5	5
Eu	0.1	1.1	0.7	1.2	0.8	1.1	0.4	0.1	1.1	0.8	0.1
Gd	3.8	7.8	4.6	5.6	5.3	4.6	5.1	4.1	4.5	3.8	5.2
Tb	0.6	1	0.7	0.8	0.8	0.7	0.7	0.6	0.6	0.5	0.8
Dy	3.7	5.7	4.2	4.4	5.1	3.8	4.3	3.5	3.8	3.5	4.6
Ho	0.7	1.1	0.9	0.9	1	0.8	0.8	0.8	0.7	0.7	1
Er	2.1	3.4	2.6	2.6	3.2	2.3	2.6	2.2	2.1	2.1	2.9
Tm	0.3	0.5	0.4	0.4	0.5	0.3	0.4	0.3	0.3	0.3	0.4
Yb	1.9	3.4	2.5	2.6	3.2	2.3	2.5	2.2	2	2	2.8
Lu	0.3	0.5	0.4	0.4	0.5	0.3	0.4	0.3	0.3	0.3	0.4
Y	20.4	30.7	22.5	23.3	30.2	21.6	23.4	19.6	18.2	16.4	26.6
Hf	4	4	5	5	4	5	5	5	3	2	2
Zr	117	115	139	179.5	123.5	164	161.5	175.5	90	77.6	71.6
Zn	96	70	62	69	68	68	127	118	79	63	114
Ga	19	10	17	19	10	18	22	20	19	16	18
Se	5	3	2	2	2	6	3	4	3	1	2
W	9	5	3	4	14	217	8	5	289	1	3
Eu/Eu*	0.1	0.4	0.5	0.7	0.5	0.7	0.2	0.1	0.7	0.7	0
La/Sm	4.9	13.4	5.2	8.7	3.4	8.4	7.3	7.3	6.4	5.6	4.8

Table 1 (Continued)

Sample	Microgranodioritic enclaves			Monzogranites							
	AGH2	EA24	AD	G22	AG19	GM11	AB6	AG16	G24	GM10	G23
SiO ₂	64.2	62.3	55	75.1	73.7	71.4	71.1	70.8	70.7	70	69.7
TiO ₂	0.7	0.6	0.8	0.1	0.3	0.3	0.2	0.4	0.2	0.3	0.2
Al ₂ O ₃	15.7	16.7	10.5	12.0	12.0	14	14.5	13.5	14.6	14.1	14.9
Fe ₂ O ₃ *	6	6.2	7.7	1.1	2.2	3	2	2.8	2.2	3.5	2.6
MnO	0.1	0.1	0.1	0	0.1	0.1	0	0.1	0.1	0.1	0.1
MgO	1.8	2.4	2.3	0.1	0.4	0.6	1.2	0.6	0.4	0.7	0.5
CaO	3.6	3.4	1.8	0.5	0.9	1.8	0.9	1	1.7	2.1	1.8
Na ₂ O	3.3	3.3	2.5	3.7	3.8	3	4.2	3.9	3.8	2.8	4.1
K ₂ O	2.2	2.7	0.3	4.6	3.0	4.1	2.1	4.1	4.6	4	4.2
P ₂ O ₅	0.3	0.1	0.1	0	0.1	0.1	0.1	0.1	0	0.1	0
Ni	22	19	46	7	7	11	13	20	9	12	8
Cr	100	100	130	130	10	20	150	10	80	20	110
Co	14.2	14.2	14.6	1.2	54.1	32.9	3.3	54.7	3.7	53.4	3.5
V	64	130	173	3.3	17	24	25	27	11	28	11
Cs	9.5	7	10.3	3.7	0.8	2.7	2.3	1.1	4.5	6.2	4.5
Rb	162.5	149.5	290	189	129	146.5	63.8	123.5	157	166.5	152.5
Sr	280	294	205	27.8	121.5	229	114	168	124.6	239	132.5
Ba	353	290	1105	38.5	320	399	276	631	438	404	372
Th	17	16	14	19	31	15	16	32	11	20	13
U	1.9	3	1.7	3.8	5.8	2.6	2.5	5.3	2.4	2.7	2.6
Ta	1.7	0.9	1	1.5	3.2	1.4	1.1	2.6	0.9	1.4	1.1
Nb	19	12	14	9	32	11	10	28	10	11	11
La	37.3	37.7	30.5	7.3	42.7	32.9	32.5	59.5	20.1	39.7	25.1
Ce	74.7	71.3	63.5	18	74.5	64.5	64.1	101.6	40.5	77.4	54.5
Pr	7.8	7.8	6.8	2.4	7.2	6.9	6.5	9.7	4.2	6.3	5.6
Nd	27.2	27.1	24.2	9.8	23	23.7	22.3	29.6	16	26.7	20.3
Sm	5.4	4.7	4.7	4	4.5	4.5	4.5	5.2	3.3	5.2	4.4
Eu	1.1	0.8	1.4	0.1	0.9	0.7	0.7	0.1	0.4	0.5	0.2
Gd	5.8	4.9	3.8	5.7	4.6	4.1	4.2	5.3	3.6	5.1	4.2
Tb	0.8	0.6	0.4	1.2	0.7	0.6	0.6	0.7	0.6	0.7	0.6
Dy	5.2	3.2	2.4	8.8	4.2	3.5	3.7	4	3.5	3.9	4.1
Ho	1	0.6	0.5	2	0.8	0.7	0.7	0.8	0.7	0.8	0.6
Er	3	1.8	1.4	6	2.5	1.9	2.2	2.5	2.1	2.2	2.7
Tm	0.5	0.2	0.2	1	0.4	0.3	0.3	0.4	0.3	0.3	0.4
Yb	3.1	1.6	1.3	5.6	2.9	2	2.4	2.6	2.1	2.2	2.6
Lu	0.4	0.2	0.2	0.9	0.4	0.3	0.3	0.4	0.3	0.3	0.4
Y	27.2	17.1	12.7	69.5	22.8	19.2	20.2	22.8	20.3	21	23.3
Hf	7	5	5	4	5	4	4	6	4	4	5
Zr	235	145.5	157.5	81.5	179	116.5	106	230	128	137	149
Zn	56	53	69	16	30	29	13	79	39	35	47
Ga	24	20	22	16	19	17	17	20	17	17	17
Se	2	1	4	3	3	2	3	4	2	2	4
W	6	4	2	8	469	225	8	416	11	429	11
Eu/Eu*	0.6	0.5	1	0	0.6	0.5	0.5	0	0.4	0.3	0.1
La/Sm	8	15.8	15.7	0.7	9.8	11	9.1	15.3	6.4	12.1	6.5

5. Geochemical characteristics

The SiO₂ content of samples vary from 52 to 75 wt% (Table 1). Most samples form near-linear to curvilinear trends of decreasing Al₂O₃, Fe₂O₃*, MnO, TiO₂, MgO, CaO and P₂O₅, and increasing K₂O and Na₂O with increasing SiO₂ (Fig.3). The patterns of these in the TiO₂ versus SiO₂ and P₂O₅ versus SiO₂ diagrams show marked inflections

at approximately 60 wt% SiO₂ and provide a slightly convex curve in the Al₂O₃ versus SiO₂ diagram. These patterns suggest that fractionation of hornblende, a Ti-bearing phase, and apatite may have played roles in these rocks.

Harker diagrams of the major elements (Fig. 3) indicate some trends suggesting clearly that the granodiorites and monzogranites may be co-magmatic, whereas the quartz-diorites seems to be derived from different source or magmatic processes.

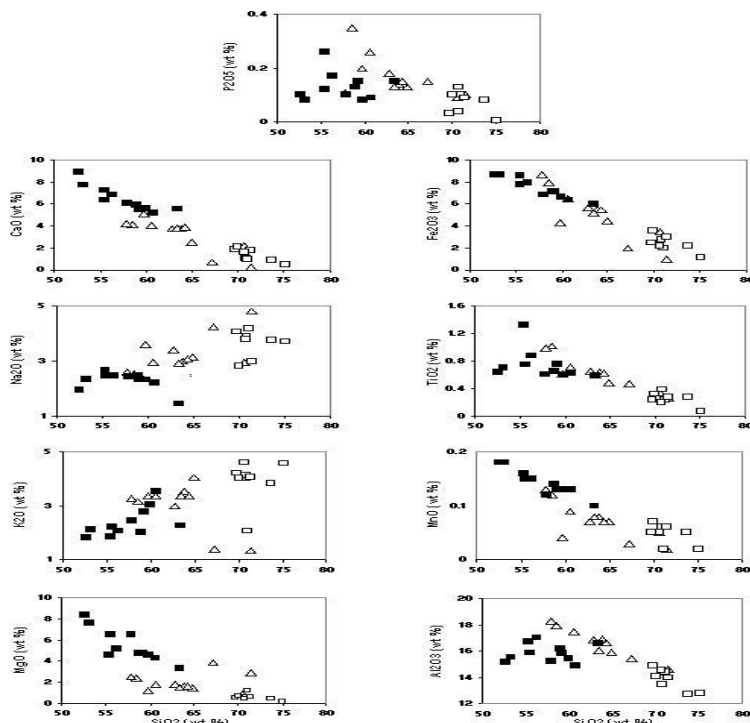


Figure 3. Harker diagrams for major elements of the Boroujerd Granitoid Complex.

Symbols: ■ quartz diorite, □ monzogranite, Δ granodiorite

The trace elements behave in a similar way when plotted versus increasing SiO₂ content (Fig.4): decreasing trends for Ba, Sr, V, Cr, Ni, Co and Zn and increasing trends for Rb, U, Ta and Nb. As was observed for the major elements, the Quartz-diorites define a distinct domain in the trace element diagrams, clearly shown by the Cr, Rb and Zr variations, suggesting a different source (or magmatic processes) for them. Transition elements (Ni, Cr, Co, V) decrease with increasing SiO₂ content, in agreement with their incorporation into early-crystallized ferromagnesian silicates. Average Nb contents are always low (<20 ppm) as it is usual in calc-alkaline rocks.

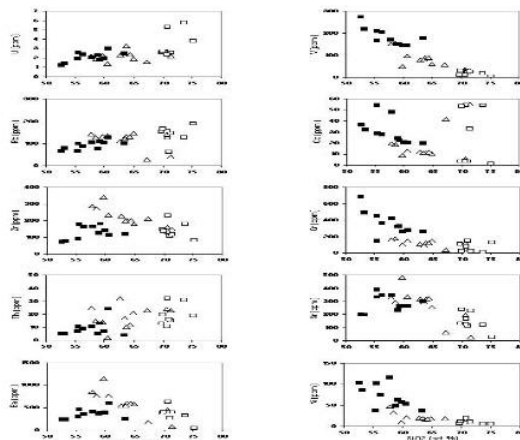


Figure 4. Harker diagrams for selected trace elements of the Boroujerd Granitoid Complex. Symbols as in Fig. 3

In the molecular $Al_2O_3/(CaO + Na_2O + K_2O)$ versus $Al_2O_3/(Na_2O + K_2O)$ [A/CNK vs. A/NK] diagram (Shand, 1947) the composition of quartz-diorites plot into the metaluminous field, while the granodiorites and the monzogranites plot into the peraluminous domain. Nevertheless, the ratio of the molecular A/CNK of the quartz-diorites as well as the most of the granodiorites and the monzogranites are in the 1 – 1.1 interval of A/CNK (Fig. 5), hence the rocks are of I-type in the sense of Chappell and White (1974). All samples are of subalkaline affinity and belong to the calc-alkaline series on the basis of the Irvine and Baragar (1971) classification scheme (fig. 6a) and show high-K affiliation based on the K_2O vs. SiO_2 diagram of Rickwood (1989) (Fig. 6b). Some of the samples (MA₃, GM₅ and AB₆) fall in the medium-K calc-alkaline field and their K_2O contents are inconsistent with their silica contents could be due to some hydrothermal alteration.

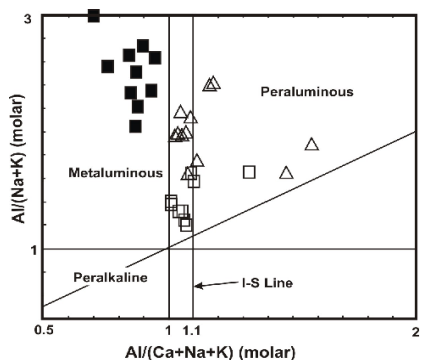


Figure 5. Molar A/CNK [$Al_2O_3/(CaO + Na_2O + K_2O)$] vs. A/NK [$Al_2O_3/(Na_2O + K_2O)$] diagram

(Shand, 1947) for the Boroujerd Granitoid Complex. Symbols as in Fig.3.

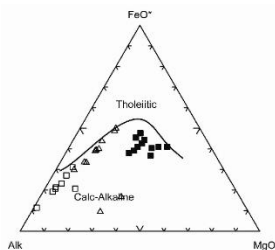


Figure 6 (a)

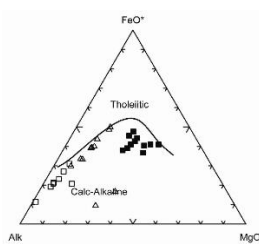


Figure .6 (a)

Figure 6. (a) K_2O vs. SiO_2 diagrams with field after Rickwood (1989): (b) AFM diagram with field delineated after Irvine and Baragar (1971). Symbols as in Fig. 3

Also, trace elements distribution patterns of the granodiorites, quartz-diorites and the monzogranites from the Boroujerd complex are normalized to primitive mantle of Sun and McDonough (1989) (Fig. 7). Accordingly, all studied samples show Eu, Nb, Ti, P and Sr depletion and are enriched in LILE (Ce, K, and Th). In comparison with HFSE (Nb, Zr, Sm, Y, and Yb), the LREE (La,Ce, Nd) show enrichment. High Ce, Th, K and low Sr, P and Ti values are compatible with typical crustal melts (Harris et al., 1986; Chappell and White, 1992).

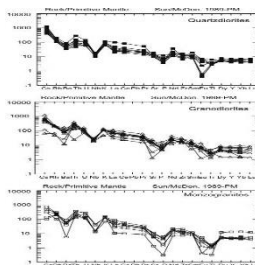


Figure 7. Primitive mantle -normalised, trace element abundance diagrams (spider diagrams) for representative samples of the studied Granitoid Complex. Normalization factors are from Sun and McDonough (1989). Symbols as in Fig. 3

Chondrite-normalized REE patterns are shown in Fig. 8. Using chondrite-normalizing values of Nakamura (1974) for REE, the light REE (LREE) patterns show enrichment for The Boroujerd granitoid complex. The samples of the granodiorites exhibit strongly fractionated REE patterns ($[La/Yb]_n = 7-53$), in which variable Eu anomalies ($Eu/Eu^* = 0.2-1.1$) and flat heavy REE (HREE) patterns are visible. The samples of the quartz-diorites again show moderately fractionated REE patterns ($[La/Yb]_n = 3-13$), but flatter heavy REE patterns with moderate negative Eu anomalies ($Eu/Eu^* = 0-0.7$). The samples of the monzogranites are characterized by strongly fractionated and flatter heavy REE patterns than the quartz diorites ($[La/Yb]_n = 5-15$) and have strong to moderate negative Eu-anomalies ($Eu/Eu^* = 0-0.6$).

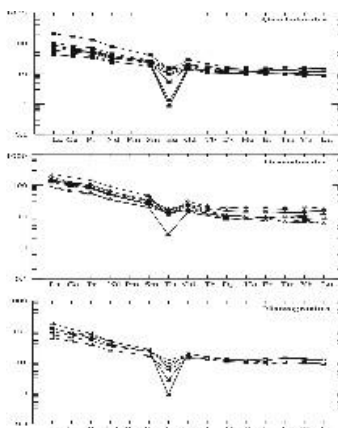


Figure 8. Chondrite-normalized REE patterns (values from Nakamura, 1974). Symbols as in Fig. 3

RESULTS AND DISCUSSION

5. Discussion

5.1. Petrogenesis

The quartz-dioritic samples and the most of the granodioritic and monzogranitic samples of the Boroujerd granitoids belong to the I-type granites of Chappell and White (1974). The S-type affinity shown by a few samples of the Boroujerd granitoids may also represent highly fractionated I-type granites, as these rocks commonly reach and even slightly exceed aluminum saturation (Chauris, 1991; Chappell, 1999) or it is due to the contamination by reaction with country rocks.

Regarding the origin of felsic arc magmas, two petrogenetic models have been proposed. According to the first model, felsic arc magmas are derived from basaltic parent magmas by Assimilation and Fractional Crystallization (AFC) processes (e.g. Grove and Donnelly-Nolan, 1986; Bacon and Druitt, 1988) or Melting, Assimilation, Storage and Homogenisation (MASH) processes (Hildreth and Moorbath, 1988). The MASH model applies to entire magma generation. Mantle and crustal magmas mixing close to the mantle-crust boundary, establish the characteristic chemical signature of magmas at the melting stage. The age and consequent chemical composition of the lower crustal component controls the isotopic variations during the assimilation stage. Finally, AFC processes may substantially modify the composition of the ascending magmas, resulting in the homogenisation stage (Hildreth and Moorbath, 1988). In the second model, basaltic magmas provide heat for the partial melting of crustal rocks (e.g. Bullen and Clyne, 1990; Roberts and Clemens, 1993; Tepper et al., 1993; Guffanti et al., 1996). The mantle is also the heat source that controls crustal melting (Vigneresse, 2004). Other mechanisms for crustal melting require either

advective or diffusive heat. Heat transfer by the former process brings hot material from the mantle and rapidly heats up the crust (Vigneresse, 2004). Due to the low concentration of the transitional elements (Ni, Cr, Co, V), the large volume of the granitoid rocks and the absence of rocks with basaltic compositions (all samples have SiO₂ content > 52%, Table 1), in the Boroujerd area, suggest that a basaltic parent magma unlikely and that the voluminous felsic magmas were generated by differentiation of mantle-derived mafic magmas. It seems also unlikely that these granitoids prove mixtures of basaltic and granitic magmas, as mixing evidences (e.g. coeval basaltic members) are lacking in the Boroujerd area.

In addition, the Boroujerd granitoids are high-K, I-type, calc alkaline rocks, characterized by pronounced negative Ba, Sr, Nb, P and Ti anomalies, enriched in Th, K, Ce, La and Nd, and have $\epsilon_{Nd}(170)$ values of -3.62 to -3.02 and the ⁸⁷Sr/⁸⁶Sr initial isotopic ratios of 0.7062 - 0.7074 (Ahmadi khalaji, 2006). The abundance of incompatible elements (K, Th, U, La, Ce) and the negative Eu anomaly support an intra crustal origin for the granitoids of the Boroujerd area. In conclusion, it could be suggested that the Boroujerd granitoids originated by partial melting of crustal protoliths having different compositions in a deforming active margin. In such a setting, mantle melts emplaced into the lower crust, most likely is the supplier for the heat required for crustal anatexis.

Fractional crystallization of the melts en route to higher crustal levels can generate the whole spectrum of granitoid types represent in the Boroujerd area. Increases in Na₂O, K₂O and decreases in TiO₂, Fe₂O₃, CaO, MgO, MnO, P₂O₅ and Al₂O₃ contents shown in the granitoids are compatible with their evolution through fractional crystallization processes (Fig. 3). Negative Ba and Sr anomalies in rocks from the Boroujerd area are associated with negative Eu anomalies, indicating evolution by fractionation of K-feldspar and plagioclase either in magma chambers or during magma ascent. This is also supported by negative correlations between CaO, Al₂O₃, and SiO₂ (Fig. 3). The fractionation of plagioclase has played an important role in the petrogenesis of the Boroujerd granitoids, as indicated by significant anomalies of Eu, Ba, and Sr (Figs. 7 and 8). Decreases in P₂O₅ with increasing SiO₂ content are attributed to fractionation of apatite (Fig. 3). The unfractionated HREE (and Y) patterns (Fig. 7) suggest that the magma was produced outside the garnet stability field whereas the negative Eu and Sr anomalies (Figs. 7 and 8) could indicate that plagioclase was stable in the source.

5.2. Tectonic setting of magma generation and emplacement

The Boroujerd Granitoid Complex is typically formed of a high-K calc-alkaline suite (Fig. 6b), in which granodiorite, quartz diorite and monzogranite are the dominant rock types. Field relations, petrography and geochemistry these rocks show similarity to intrusions typical of the active continental margins. Numerous studies suggest that trace elements can be used to discriminate between the different tectonic settings of granitoid magmas (e. g. Pearce, 1983; Pearce et al. 1984; Harris et al., 1986); although they must be used with caution as they could represent the formation of the protoliths rather than those of the derived magma. The Boroujerd granitoids in the geotectonic classification of Pearce et al. (1984) are classified as volcanic arc granites (Fig. 9). Furthermore, as discussed earlier, granitoids of the Boroujerd area are enriched in LILE such as Cs, K, Rb, and Th with respect to the HFSE, especially Nb and Ti (Fig. 7). Magmas with these geochemical characters are generally ascribed to the subduction-related environments (e.g., Rogers and Hawkesworth 1989; Sajona et al. 1996). High Th/Yb ratios correlated with high values for La/Yb are consistent with continental arc magmas (Fig. 10)

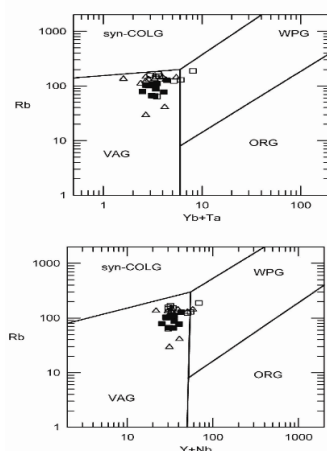


Figure 9. Rb vs. (Yb + Ta) and Rb vs. (Y + Nb) diagrams of Pearce et al. (1984); ORG, ocean-ridge granites; syn-COLG, syn-collisional granites; VAG, volcanic arc granites; WPG, within-plate granites. Symbols as in Fig. 3

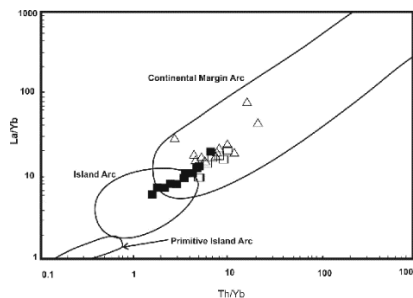


Figure 10. La/Yb vs. Th/Yb diagram after Condie (1989). Symbols as in Fig. 3

CONCLUSION

The Boroujerd Granitoid Complex is made of three units including quartz diorite, granodiorite and monzogranite. The geochemical characteristics, mineralogy and petrography of these rocks are comparable with the typical I-type granites. The Complex belongs to metaluminous to slightly peraluminous, a high-K calc-alkaline series, and displays geochemical characteristics typical of volcanic arc granites related to an active continental margin. The geochemical data for the Boroujerd granitoids are consistent with derivation from a crustal source and it could be suggested that the granitoids originated by partial melting of crustal protoliths having different compositions in a deforming active margin. This conclusion is in good agreement with the general model of Berberian (1983) and Shahabpour (2005) which assumed that the Sanandaj-Sirjan calc-alkaline magmatic arc formed over a high angle subducting oceanic slab in the Neotethyan subduction zone during Late Triassic to Late Cretaceous time.

REFERENCES

- Book chapter: Ahmadi Khalaji A. 2006. Petrology of the granitoid rocks of the Boroujerd area. PhD Thesis, University of Tehran, Tehran, Islamic Republic of Iran pp190.
- Book chapter: Masoudi F. 1997. Contact metamorphism and pegmatite development in the SW of Arak, Iran. PhD thesis, The University of Leeds, UK 231
- Book chapter: Grove TL and Donnelly-Nolan JM. 1986. The evolution of young silicic lavas at Medicine lake Volcano, California: implications for the origin of compositional gaps in calc-alkaline series lavas. *Contribution to Mineralogy and Petrology* 92: 281–302
- Book chapter: Berberian M. 1983. Generalized tectonic map of Iran. In: Berberian, M., (Ed.), *Continental Deformation in the Iranian Plateau*, Geological Survey of Iran, Report 52
- Book chapter: Berberian F and Berberian M. .1981. Tectono-plutonic episodes in Iran. In: Gupta, H.K., Delany, F.M. (Eds.), *Zagros Hindukosh, Himalaya Geodynamic Evolution*, American Geophysical Union, Washington, DC 5–32
- Book chapter: Berberian M. 1977. Three phases of metamorphism in Haji-Abad quadrangle (southern extremity of the Sanandaj–Sirjan structural Zone): a palaeotectonic discussion. In: M. Berberian, (Ed.), *Geological Survey of Iran, Report 40*, Tehran, Iran pp. 239–263
- Book chapter: Isacks B and Barazangi M. 1977. Geometry of Benioff Zones: lateral segmentation and downwards bending of the subducted lithosphere. In: *Island arcs, deep sea trenches and back arc basins*, Maurice Ewing Series 1, American Geophysical Union 99–114
- Book chapter: Berthier F and Billiaul HP. 1974. Etude Stratigraphique, petrologique et structural de La region de khorrabad (zagros, Iran). These de 3e cycle, Grenoble 282
- Book chapter: Shand SJ. 1947. *Eruptive Rocks*, D. Van Nostrand Company, New York 360
- Journal article: Bacon CR and Druitt TH. 1988. Compositional evolution of the zoned calcalkaline magma chamber of Mt. Mazama, Crater Lake, Oregon. *Contributions to Mineralogy and Petrology* 98: 224–256
- Journal article: Baharifar A and Moinevaziri H. 2004. The crystalline complexes of Hamadan (Sanandaj–Sirjan zone, western Iran): metasedimentary Mesozoic sequences affected by Late Cretaceous tectono-metamorphic and plutonic events. *C. R. Geoscience* 336: 1443-1452
- Journal article: Bullen TD and Clyne MA. 1990. Trace element and isotopic constraints on magmatic evolution at Lassen volcanic center. *Journal of Geophysical Research* 95: 19671–19691
- Journal article: Chappell BW. 1999. Aluminium saturation in I- and S-type granites and the characterization of fractionated haplogranites. *Lithos* 46: 535-551
- Journal article: Chappell BW and White AJR. 1974. Two contrasting granite types. *Pacific Geology* 8: 173–174
- Journal article: Chappell BW and White AJR. 1992. I and S-type granites in the Lachlan Fold Belt. *Transactions of the Royal Society of Edinburgh: Earth Sciences* 83: 1–26
- Journal article: Chauris L. 1991. Le granite a tourmaline de plouarzel (Finistere) : aspects chimico- mineralogiques dune differentiation marginale leocogranitique. *Geologie de la France* 4: 31-38

- Journal article: Condie KC. 1989. Geochemical changes in basalts and andesites across the Archean–Proterozoic boundary: identification and significance. *Lithos* 23: 1–18
- Journal article: Cotten J and Le Dez A. 1995. Origin of anomalous rare earth element and yttrium enrichment in subaerially exposed basalts: evidence from France Polynesia. *Chemical Geology* 119: 115-138
- Journal article: Guffanti M and Clynne MA. 1996. Thermal and mass implications of magmatic evolution in the Lassen volcanic region, California, and constraints on basalt influx to the lower crust. *Journal of Geophysical Research* 101: 3001–3013
- Journal article: Harris NBW and Pearce JA. 1986. Geochemical characteristics of collision-zone magmatism. In: Coward, M.P., Ries, A.C. (Eds.), *Collision Tectonics*. Geological Society London, Special Publication 19: 67–81
- Journal article: Hildreth EW and Moorbat S. 1988. Crustal contributions to arc magmatism in the Andes of Central Chile. *Contribution to Mineralogy and Petrology* 76: 177–195
- Journal article: Irvine TN, Baragar WRA. 1971. A guide to the chemical classification of the common volcanic rocks. *Canadian Journal of Earth Sciences* 8: 523-548
- Journal article: Mohajjel M and Fergusson CL. 2003. Cretaceous–Tertiary convergence and continental collision, Sanandaj-Sirjan Zone, Western Iran. *Journal of Asian Earth Sciences* 21: 397–412
- Journal article: Nakamura N. 1974. Determination of REE, Ba, Fe, Mg, Na, and K in carbonaceous and ordinary chondrites. *Geochimica et Cosmochimica Acta* 38: 757–775
- Journal article: Pearce JA and Harris NBW. 1984. Trace element discrimination diagrams for the tectonic interpretation of granitic rocks. *Journal of Petrology* 25: 956–983
- Book chapter: Pearce JA. 1983. Role of the sub-continental lithosphere in magma genesis at active continental margins. In: Hawkesworth, C.J., Norry, M.J. (Eds.), *Continental Basalts and Mantle Xenoliths*. Shiva Publishing, Nantwich 158–185
- Journal article: Rickwood PC. 1989. Boundary lines within petrologic diagrams which use of major and minor elements. *Lithos* 22: 247–263
- Journal article: Roberts MP and Clemens JD. 1993. Origin of high-potassium, calc-alkaline, I-type granitoids. *Geology* 21: 825–828
- Journal article: Rogers G and Hawkesworth CJ. 1989. A geochemical traverse across the North Chilean Andes: evidence for crust generation from the mantle wedge. *Earth and Planetary Science Letters* 91: 271–285
- Journal article: Sajona FG and Maury RC. 1996. High field strength elements of Pliocene-Pleistocene island-arc basalts Zamboanga Peninsula, Western Mindanao (Philippines). *Journal of Petrology* 37: 693–726
- Journal article: Shahabpour J. 2005. Tectonic evolution of the orogenic belt in the region located between Kerman and Neyriz. *Journal of Asian Earth Sciences* 24: 405-417
- Journal article: Stöcklin J. 1968. Structural history and tectonics of Iran; a review. *American Association of Petroleum Geologists Bulletin* 52: 1229–1285
- Journal article: Sun SS and McDonough WF. 1990. Chemical and isotopic systematics of oceanic basalts: implications for mantle composition and processes. In: Saunders, A.D., and Norry, M.J. (eds.), *Magmatism in ocean basins*. Geological Society London, Special Publication 42: 313–345
- Journal article: Tepper JH and Nelson BK. 1993. Petrology of the Chilliwack batholith, North Cascades, Washington: generation of calc-alkaline granitoids by melting of mafic lower crust with variable water fugacity. *Contribution to Mineralogy and Petrology* 113: 333–351
- Vigneressse JL. 2004. A new paradigm for granite generation. *Transactions of the Royal Society of Edinburgh: Earth Sciences* 95, 11-22.